LETTERS

Non-equilibrium degassing and a primordial source for helium in ocean-island volcanism

Helge M. Gonnermann[1]† & Sujoy Mukhopadhyay[1]

Radioactive decay of uranium and thorium produces ^{4}He, whereas ^{3}He in the Earth's mantle is not produced by radioactive decay and was only incorporated during accretion—that is, it is primordial[1]. ^{3}He/^{4}He ratios in many ocean-island basalts (OIBs) that erupt at hotspot volcanoes, such as Hawaii and Iceland, can be up to sixfold higher than in mid-ocean ridge basalts (MORBs). This is inferred to be the result of outgassing by melt production at mid-ocean ridges in conjunction with radiogenic ingrowth of ^{4}He, which has led to a volatile-depleted upper mantle (MORB source) with low ^{3}He concentrations and low ^{3}He /^{4}He ratios[2–6]. Consequently, high ^{3}He/^{4}He ratios in OIBs are conventionally viewed as evidence for an undegassed, primitive mantle source, which is sampled by hot, buoyantly upwelling deep-mantle plumes[3,6,7]. However, this conventional model provides no viable explanation of why helium concentrations and elemental ratios of He/Ne and He/Ar in OIBs are an order of magnitude lower than in MORBs. This has been described as the 'helium concentration paradox'[8] and has contributed to a long-standing controversy about the structure and dynamics of the Earth's mantle. Here we show that the helium concentration paradox, as well as the full range of noble-gas concentrations observed in MORB and OIB glasses, can self-consistently be explained by disequilibrium open-system degassing of the erupting magma. We show that a higher CO_2 content in OIBs than in MORBs leads to more extensive degassing of helium in OIB magmas and that noble gases in OIB lavas can be derived from a largely undegassed primitive mantle source.

The high ^{3}He/^{4}He ratios in OIBs form the cornerstone of the conventional view that parts of the deep mantle have been isolated from outgassing and the convective upper mantle over Earth's history[5]. Preservation of an undegassed mantle reservoir is, however, difficult to reconcile with whole-mantle convection. In conjunction with the helium concentration paradox[8] this has led to alternative interpretations of high ^{3}He/^{4}He ratios in OIBs. For example, high ^{3}He/^{4}He ratios have been assigned to recycled lithosphere instead of primitive mantle[9] and it has been suggested that high ^{3}He/^{4}He ratios in OIBs indicate low ^{4}He rather than high ^{3}He concentrations[10]. Distinguishing between these and similar hypotheses is fundamental to our understanding of mantle dynamics and the origin of chemical heterogeneities in the mantle.

Because primitive mantle has considerably higher primordial noble-gas concentrations than the MORB mantle source[1], OIBs are expected to have higher ^{3}He concentrations than MORBs, but similar He/Ne and He/Ar elemental ratios[1,11]. However, it has been known for more than two decades that most OIB samples have significantly lower helium concentrations and also elemental ratios than MORBs[12]. This apparent discrepancy, the helium concentration paradox, cannot be explained by existing models of magma degassing[13,14] (Fig. 1). Constraining the ^{3}He concentration in parental (that is, undegassed) OIB magma can provide a critical test for the presence of a primitive component in the OIB mantle source. Here we present a new, self-consistent model for degassing of CO_2, H_2O and noble gases (^{3}He, ^{4}He, ^{22}Ne, ^{21}Ne and ^{40}Ar) in OIB and MORB magmas, which resolves the helium concentration paradox and constrains the noble-gas concentrations in the parental magmas.

Volatile solubilities decrease during ascent-driven magma decompression, resulting in the growth of gaseous bubbles. If there is sufficient time for volatiles to diffuse from the melt into bubbles, the concentration of dissolved volatiles will be in equilibrium with the coexisting bubbles and the process is called equilibrium degassing. Degassing can be further classified as open-system or closed-system, depending on whether or not the exsolved bubbles are lost from the

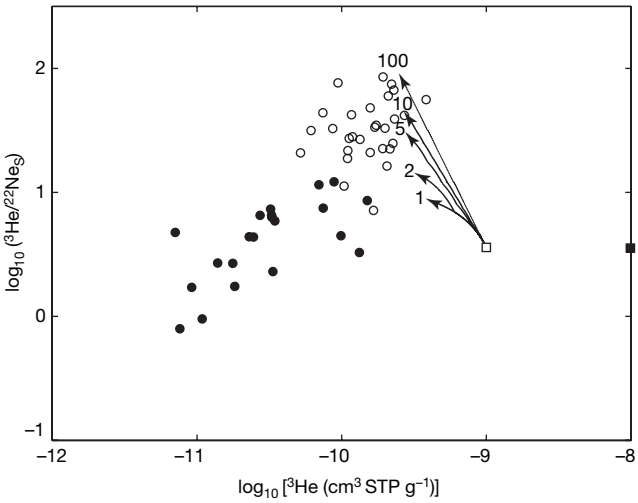

Figure 1 | Equilibrium degassing trajectories. Open and filled circles are MORB and OIB step heating analyses of submarine glasses, respectively (details are given in Supplementary Information). $^{22}Ne_S$ is the mantle-derived primordial neon obtained by correcting the measured ^{22}Ne for atmospheric contamination[11]. Both the elemental ratio, $^3He/^{22}Ne_S$, and ^{3}He concentrations in OIBs are considerably lower than in MORBs, contrary to expectations for OIBs derived from a primitive mantle source. Initial ^{3}He is 10^{-9} cm^3 STP g^{-1} (ref. 1). Curved arrows represent degassing paths for the melt. The shortest degassing path is for a closed-system equilibrium case (one degassing step). The remaining trajectories are for 2-step, 5-step, 10-step and 100-step open-system equilibrium degassing models. For details on degassing calculations see the text and Supplementary Information. ^{3}He concentration for undegassed OIB (filled square) is one order of magnitude higher than for MORB (open square). Starting from undegassed OIB will simply shift the degassing trajectories to the right and therefore none of the equilibrium degassing models can explain the low $^3He/^{22}Ne_S$ or the low ^{3}He concentrations in OIBs.

[1]Department of Earth and Planetary Sciences, Harvard University, Cambridge, Massachusetts 02138, USA. †Present address: Department of Geology and Geophysics, SOEST, University of Hawaii, Honolulu, Hawaii, 96822, USA.

magma during ascent and eruption. Most MORBs and OIBs are thought to erupt by means of open-system degassing[15,16]. During equilibrium degassing, elemental fractionation is controlled solely by the relative solubilities of the volatile species. Because noble-gas solubility decreases with increasing atomic size[17], He/Ar and He/Ne ratios always increase during equilibrium degassing and neither open-system nor closed-system equilibrium degassing can explain why erupted OIB lavas have elemental ratios lower than the starting composition[13,14] (Fig. 1). This is a fundamental problem, which any successful degassing model needs to explain, and is independent of whether the OIB mantle source has a higher volatile content than the MORB source.

Recent work has suggested that differences in diffusivity between noble gases may also lead to elemental fractionation in MORBs[16,18,19], in a process called disequilibrium degassing[20]. We propose that the difference in noble-gas concentrations and elemental ratios between MORBs and OIBs is a result of disequilibrium degassing. Disequilibrium degassing kinetically limits diffusive gas loss from the melt, and the dissolved concentrations of slowly diffusing volatiles may remain above equilibrium during degassing (Fig. 2). The magnitude of kinetic fractionation depends on magma vesicularity, bubble size and t_{degas}, the time available for degassing, which we express in terms of $\tau_{Ar} = a^2/D_{Ar}$, the characteristic diffusion time of argon in basalt melt. Here $D_{Ar} = 10^{-11.5}\,m^2\,s^{-1}$ is argon diffusivity and $a = R(\phi^{-1/3} - 1)$ is the characteristic thickness of melt surrounding bubbles of radius R at a vesicle volume fraction ϕ. Kinetic fractionation of noble gases depends on relative diffusivities, which to first order scale as $D_{Ar} \sim D_{Ne} \sim 0.01 D_{He}$ (details are given in Supplementary Information). In other words, $\tau_{Ar} \sim \tau_{Ne} \sim 100\tau_{He}$ and if $\tau_{Ar} > t_{degas} > 0.01\tau_{Ar}$, then helium will be lost from the melt as pressure and, hence, solubility decrease. At the same time degassing of argon and neon will be limited by the ability of these gases to diffuse out of the melt. As a result, disequilibrium degassing will lead to He/Ne and He/Ar ratios in the erupted lavas that are lower than the starting composition (Fig. 2).

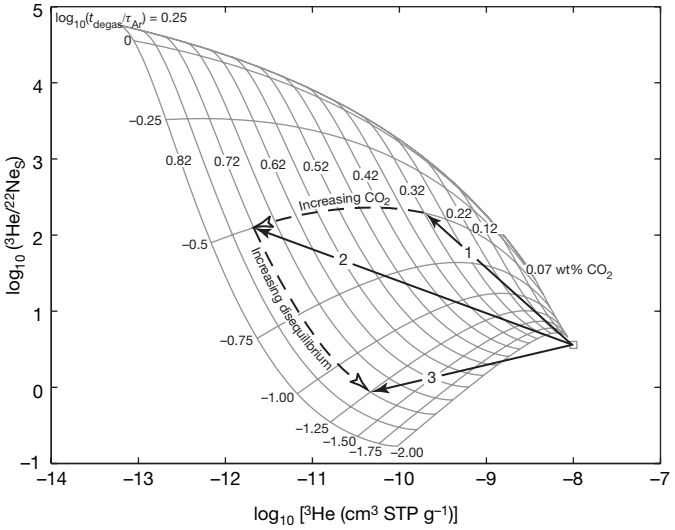

Figure 2 | Conceptual framework of our disequilibrium degassing model. Field of possible solutions for a degassing model with ten steps of open-system gas loss, an eruption depth of 5,500 m below sea level, and incorporating the effect of major volatiles on degassing at 55 MPa. Any point that falls within the solution grid represents the calculated dissolved noble-gas content of the degassed melt for a specific initial CO_2 and H_2O content and degassing time, but at a constant pressure. Because H_2O solubility is much higher than CO_2 solubility[21], most H_2O remains dissolved on eruption and does not significantly affect model results. We therefore always set initial H_2O content equal to initial CO_2. Degassing times are expressed in terms of the characteristic diffusion time of argon (the slowest diffusing noble gas under consideration) in basalt melt, τ_{Ar}. If t_{degas}, the time available for degassing during magma eruption, is similar to τ_{Ar}, the characteristic diffusion time of argon, then the degassing calculations are close to equilibrium. If $t_{degas} \ll \tau_{Ar}$, there is insufficient time for diffusion of argon (and also neon, because of its low diffusivity) and degassing is in disequilibrium. Because τ_{Ar} represents an e-folding time, concentrations are essentially at equilibrium for $\log_{10}(t_{degas}/\tau_{Ar}) > 0.25$. Subhorizontal lines are isopleths of constant degassing time relative to τ_{Ar}, with decreasing durations from top to bottom. Subvertical lines are isopleths of constant initial CO_2 (H_2O) with increasing concentrations from right to left. Solid arrows represent three illustrative degassing trajectories and mark the composition of the erupted lavas. Trajectories 1 and 2 have different initial CO_2 content but the same degree of disequilibrium. Trajectories 2 and 3 have the same initial CO_2 content but different degrees of disequilibrium. Note that higher initial CO_2 content leads to more helium loss from the melt (subhorizontal dashed arrow). Increasing the degree of disequilibrium, by decreasing the time available for degassing, results in lower He/Ne ratios (subvertical dashed arrow). Open square, undegassed melt.

In our model we explicitly account for the effect of CO_2 and H_2O on degassing of noble gases. Varying the major volatile content of the magma affects the partial pressures of noble gases, and hence their solubility. Because most H_2O remains dissolved in the melt at typical eruptive pressures[21], we simplify our analysis and assume that H_2O concentrations in the undegassed magma are equal to CO_2 concentrations. When both the effects of disequilibrium and major volatiles are modelled quantitatively, helium concentrations in erupted lavas decrease as initial CO_2 increases, whereas neon and argon remain relatively unaffected, resulting in low He/Ne and He/Ar ratios (Fig. 2). We also account for eruption depth, because solubility depends on pressure; a lower eruption depth will increase the magnitude of helium degassing[22]. However, variations in eruption depth alone cannot resolve the helium concentration paradox (details are given in Supplementary Information).

We apply our model of magma degassing to MORBs and OIBs to investigate whether parental magmas of OIBs can have higher noble-gas abundances than MORBs, and whether the low elemental ratios in the erupted OIB lavas are the result of disequilibrium degassing. On eruption, volatile solubilities are lowest and magma ascent rates may be sufficient for disequilibrium to occur. Thus, to provide the simplest but still insightful analysis, we model only syneruptive magma degassing. To limit the number of free parameters and facilitate direct comparison between MORBs and OIBs, we model degassing of a single representative MORB and OIB magma. For all cases we assume syneruptive, open-system degassing with ten repeated steps of gas loss at the pressure of eruption onto the sea floor. Realistic variations of all parameters (for example, number of degassing steps, solubility constants, and diffusivities) affect the details of model predictions but not the overall conclusions of our work.

Our model parental MORB and OIB magmas have $^4He/^{21}Ne$ and $^4He/^{40}Ar$ ratios equal to time-integrated production ratios of 2.22×10^7 and 2.9, respectively[11], and $^3He/^{22}Ne$ ratios of 3.6 (refs 1, 23). Although MORB and OIB mantle sources may have different $^3He/^{22}Ne$ ratios[24] and $^4He/^{40}Ar$ may vary in the parental magmas[11], we choose the same starting composition to minimize free parameters. The ^3He concentration of the parental MORB magma is $10^{-9}\,cm^3\,STP\,g^{-1}$ (cm^3 of gas at standard temperature and pressure per gram of melt) with a $^3He/^4He$ ratio of $8.1R_A$ (measured $^3He/^4He$ relative to atmospheric)[11]. Our parental MORB magma has similar noble-gas concentrations to those of popping rock, 2ΠD43 (refs 25, 26), whose unusual volatile content may be representative of undegassed MORB[27], but could also be the consequence of bubble accumulation[25].

The volatile content of the OIB mantle source is thought to include contributions from both primitive and recycled material[28]. We choose a ^3He concentration for our parental OIB magma on the basis of generating a $^3He/^4He$ ratio of $24R_A$, the average of our OIB data compilation, by mixing 80% recycled slab containing no ^3He and 20% primitive mantle with $4 \times 10^{-9}\,cm^3\,STP\,g^{-1}$ of ^3He (details are given in Supplementary Information). The resultant ^3He concentration of $10^{-8}\,cm^3\,STP\,g^{-1}$ is an order of magnitude higher than in

parental MORB. OIBs with higher $^3He/^4He$ ratios require a smaller slab component in their mantle source, resulting in higher helium concentrations, and vice versa. Within realistic ranges of initial concentrations and elemental ratios our degassing model can match the entire OIB data array (Fig. 3).

Disequilibrium in MORBs has been observed previously[16,18,19] and the entire MORB data array can be explained by disequilibrium open-system degassing. For an eruption depth of 3,500 m below sea level, Fig. 3a, b illustrates how varying the CO_2 content of the parental MORB magma and the degassing time can capture the range of observed compositions in erupted lavas. Figure 4 shows our estimate of the parental CO_2 content for individual samples. Model calculations are for an eruption depth equal to the sample depth. The CO_2 content of the parental magma and t_{degas} were calculated by varying these parameters to minimize the least-squares error of predicted to measured ^3He, ^4He, ^{21}Ne, ^{22}Ne and ^{40}Ar concentrations (details are given in Supplementary Information). Concentration estimates for CO_2 of parental MORBs range from 0.07 to 0.24 wt% with a mean of 0.13 wt%, within the range of estimates for undegassed MORBs[29,30]. Average characteristic eruption times range from $0.05\tau_{Ar}$ to $0.23\tau_{Ar}$ with a mean of $0.12\tau_{Ar}$. Within a single eruption most bubbles will span a size range of $100\ \mu m \leq R \leq 1{,}000\ \mu m$ (refs 19, 25). Reasonable values for vesicularity are $0.01 \leq \phi \leq 0.1$ (refs 19, 25). Thus, for MORBs that ascend a distance of the order of 1,000 m, kinetic fractionation of helium from neon and argon will occur at ascent rates of 0.001 to 1 m s^{-1}, within the range of estimated values[16,31].

The entire OIB data array can also be explained by open-system degassing (Fig. 3c, d) with similar degrees of kinetic fractionation to those of MORBs. Figure 4 shows our estimates for CO_2 in parental OIB magmas, which range from 0.11 to 0.63 wt% with a mean of 0.36 wt%, also within the range of measured values[15]. Characteristic degassing times range from $0.09\tau_{Ar}$ to $0.20\tau_{Ar}$ with a mean of $0.15\tau_{Ar}$. Although shallow eruption depths of some OIBs (~1,000 m below sea level) give model fits with a similar initial CO_2 content to that of MORBs, some of the deepest OIB samples (>4,500 m below sea level) have very low helium concentrations and require high CO_2 contents (Fig. 4). Thus, OIBs require, on average, a higher initial volatile content than MORBs (Fig. 4) but no other significant differences in degassing.

$CO_2/^3He$ ratios from vent fluids are commonly assumed to reflect the composition of the parental magma[32,33]. However, during degassing the $CO_2/^3He$ ratios increase as helium is lost from the magma. $CO_2/^3He$ ratios of our parental magmas are about 10^9 for MORBs and 2×10^8 for OIBs, but degassing can produce more than one order of magnitude change in $CO_2/^3He$. Fractionation of CO_2 and ^3He is larger for OIBs, as a consequence of their higher CO_2 content and resultant increase in helium loss. Therefore, even in the absence

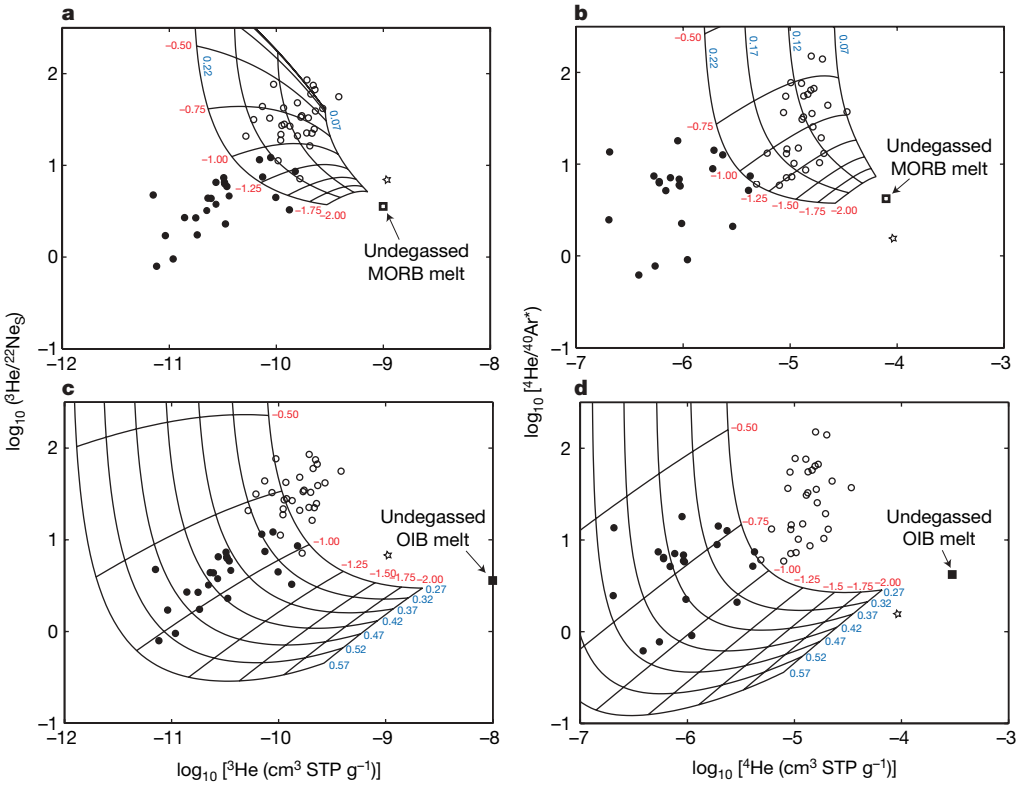

Figure 3 | Model results for disequilibrium degassing of MORBs and OIBs. **a**, **b**, Solution grid for degassing of a MORB parental melt (open square); **c**, **d**, solution grid for degassing of an OIB parental melt (filled square). CO_2 numbers on the grid represent the initial CO_2 (H_2O) content in the undegassed melt (wt% CO_2; blue numbers). Negative isopleth labels (red numbers) represent the degree of disequilibrium and are values of $\log_{10}(t_{degas}/\tau_{Ar})$. Pressure is held constant and equivalent to an eruption depth of 3,500 m below sea level. Data are identical to those in Fig. 1. **a**, Plot of $^3He/^{22}Ne_S$ against ^3He in MORBs. Disequilibrium degassing models capture the range of compositions observed in erupted MORB lavas. **b**, Plot of $^4He/^{40}Ar^*$ against ^4He in MORBs. $^{40}Ar^*$ is the mantle-derived radiogenic argon obtained by correcting the measured ^{40}Ar for atmospheric contamination[11]. The range of solutions capture the MORB data array. Overall these model results suggest that MORBs are consistent with variable degrees of disequilibrium open-system degassing at characteristic eruption times of the order of $0.1\tau_{Ar}$ from a parental MORB melt with low CO_2 and H_2O content. These results are also consistent for $^4He/^{21}Ne^*$ against ^4He (details are given in Supplementary Information). Open square, undegassed MORB melt. **c**, Plot of $^3He/^{22}Ne_S$ against ^3He in OIBs. **d**, Plot of $^4He/^{40}Ar^*$ against ^4He in OIBs. The solution grid encompasses all OIB data and produces lower noble-gas contents than erupted MORBs, as well as lower elemental ratios than the undegassed OIB melt (filled square). Solutions in He–Ar space are shifted slightly downwards relative to He–Ne space. A small decrease in $^3He/^{22}Ne_S$ of the parental OIB melt would compensate for this. Overall, our model results suggests that OIBs are consistent with disequilibrium open-system degassing with characteristic eruption times of the order of $0.1\tau_{Ar}$, and CO_2 (H_2O) contents in the parental magmas that are higher than for MORBs. These results are also consistent for $^4He/^{21}Ne^*$ against ^4He space (details are given in Supplementary Information). Open circles, MORBs; filled circles, OIBs; open star, 2ΠD43.

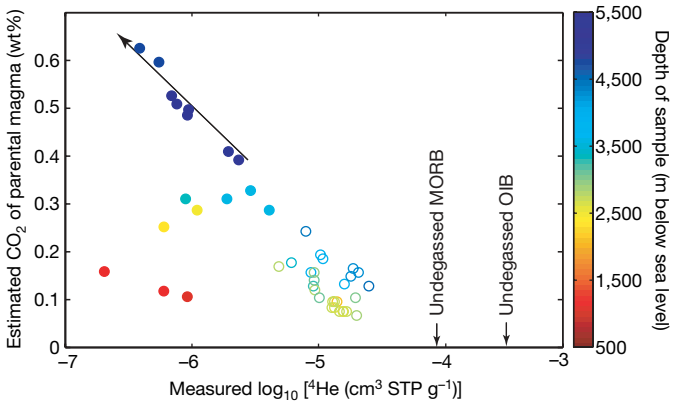

Figure 4 | Predicted CO_2 content of parental magmas. Plot of CO_2 against ^{4}He in MORBs (open circles) and OIBs (filled circles), with colours representing sample depth. Vertical arrows indicate the composition of the parental MORB and OIB magmas. Using the degassing model, we estimate the CO_2 content and degree of disequilibrium required to provide the minimum misfit (details are given in Supplementary Information) between predicted and measured noble-gas concentrations (^{3}He, ^{4}He, ^{22}Ne$_S$, ^{21}Ne* and ^{40}Ar*) for each individual sample at an eruption depth equivalent to the reported sample depth. The initial CO_2 content of MORBs ranges from 0.07 to 0.24 wt% with a mean of 0.13 wt%. The predicted CO_2 content of OIBs ranges from 0.11 to 0.63 wt% with a mean of 0.36 wt%. Overall, OIBs require a higher and wider range of initial CO_2, with concentrations up to about 0.7 wt%. Predicted eruption times (not shown) range from $0.05\tau_{Ar}$ to $0.23\tau_{Ar}$ with a mean of $0.12\tau_{Ar}$ for MORBs, and $0.09\tau_{Ar}$ to $0.20\tau_{Ar}$ with a mean of $0.15\tau_{Ar}$ for OIBs. The diagonal arrow indicates that increasing the CO_2 content of the undegassed magma decreases partial pressure and solubility of helium during degassing.

of fractionation during hydrothermal circulation[33], observed $CO_2/^3$He ratios in vent fluids and lavas may not be representative of the mantle source.

Thus, because of relatively high diffusivity, degassing of helium is not significantly limited by diffusion. Higher CO_2 content of OIBs dilutes helium in the exsolved gas phase, relative to MORBs, thereby lowering partial pressures and helium solubility. This explains why OIB lavas have lower helium abundances than MORBs, even though the OIB parental magma is more helium rich. Degassing of neon and argon is limited by diffusion in both MORBs and OIBs. In combination with higher helium loss in OIBs, this explains the low He/Ne and He/Ar ratios of OIBs relative to MORBs (Fig. 3). For example, disequilibrium open-system degassing of parental OIB magmas with noble-gas abundances of 1×10^{-8}, 2.8×10^{-9} and 7.1×10^{-5} cm^3 STP g^{-1} for ^{3}He, ^{22}Ne and ^{40}Ar, respectively, is consistent with observations (Figs 3 and 4).

We conclude that there is no helium concentration paradox. Low noble-gas concentrations and elemental ratios of OIBs are simply the consequence of disequilibrium degassing of a more volatile-rich parental magma. Our results are consistent with high ^{3}He/^{4}He ratios in OIB lavas being derived from a primitive mantle component with ^{3}He, ^{22}Ne and ^{36}Ar abundances of the order of 10^{-9} cm^3 STP g^{-1}. In agreement with some previous estimates[28], the percentage of primitive mantle in the OIB source is about 20% or less, but our calculations do not constrain its size, geometry or location. Regardless of whole-mantle convection, it seems that part of the Earth's mantle has remained largely undegassed over Earth's history.

Received 6 April; accepted 11 September 2007.

1. Porcelli, D. & Ballentine, C. J. Models for the distribution of terrestrial noble gases and evolution of the atmosphere. *Rev. Mineral. Geochem.* **47,** 411–480 (2002).
2. Hart, R., Dymond, J. & Hogan, L. Preferential formation of the atmosphere–sialic crust system from the upper mantle. *Nature* **278,** 156–159 (1979).
3. Kurz, M. D., Jenkins, W. J. & Hart, S. R. Helium isotopic systematics of oceanic islands and mantle heterogeneity. *Nature* **297,** 43–47 (1982).
4. Allègre, C. J., Staudacher, T., Sarda, P. & Kurz, M. Constraints on evolution of Earth's mantle from rare-gas systematics. *Nature* **303,** 762–766 (1983).
5. O'Nions, R. K. & Oxburgh, E. R. Heat and helium in the Earth. *Nature* **306,** 429–431 (1983).
6. Kellogg, L. H. & Wasserburg, G. J. The role of plumes in mantle helium fluxes. *Earth Planet. Sci. Lett.* **99,** 276–289 (1990).
7. Morgan, W. J. Convective plumes in lower mantle. *Nature* **230,** 42–43 (1971).
8. Anderson, D. L. The helium paradoxes. *Proc. Natl Acad. Sci. USA* **95,** 4822–4827 (1998).
9. Helfrfrich, G. R. & Wood, B. J. The Earth's mantle. *Nature* **412,** 501–507 (2001).
10. Anderson, D. L. A model to explain the various paradoxes associated with mantle noble gas geochemistry. *Proc. Natl Acad. Sci. USA* **95,** 9087–9092 (1998).
11. Graham, D. W. Noble gas isotope geochemistry of mid-ocean ridge and ocean island basalts: Characterization of mantle source reservoirs. *Rev. Mineral. Geochem.* **47,** 247–317 (2002).
12. Fisher, D. E. Noble gases from oceanic island basalts do not require an undepleted mantle source. *Nature* **316,** 716–718 (1985).
13. Honda, M. & Patterson, D. B. Systematic elemental fractionation of mantle-derived helium, neon, and argon in mid-oceanic ridge glasses. *Geochim. Cosmochim. Acta* **63,** 2863–2874 (1999).
14. Moreira, M. & Sarda, P. Noble gas constraints on degassing processes. *Earth Planet. Sci. Lett.* **176,** 375–386 (2000).
15. Dixon, J. E. & Clague, D. A. Volatiles in basaltic glasses from Loihi seamount, Hawaii: Evidence for a relatively dry plume component. *J. Petrol.* **42,** 627–654 (2001).
16. Paonita, A. & Martelli, M. A new view of the He–Ar–CO_2 degassing at mid-ocean ridges: Homogeneous composition of magmas from the upper mantle. *Geochim. Cosmochim. Acta* **71,** 1747–1763 (2007).
17. Carroll, M. R. & Stolper, E. M. Noble gas solubilities in silicate melts and glasses: New experimental results for argon and the relationship between solubility and ionic porosity. *Geochim. Cosmochim. Acta* **57,** 5039–5051 (1993).
18. Burnard, P., Harrison, D., Turner, G. & Nesbitt, R. Degassing and contamination of noble gases in Mid-Atlantic Ridge basalts. *Geochem. Geophys. Geosyst.* 4, 10.1029/2002GC000326 (2003).
19. Aubaud, C., Pineau, F., Jambon, A. & Javoy, M. Kinetic disequilibrium of C, He, Ar and carbon isotopes during degassing of mid-ocean ridge basalts. *Earth Planet. Sci. Lett.* **222,** 391–406 (2004).
20. Lensky, N. G., Navon, O. & Lyakhovsky, V. Bubble growth during decompression of magma: experimental and theoretical investigation. *J. Volcanol. Geotherm. Res.* **129,** 7–22 (2004).
21. Dixon, J. E. Degassing of alkalic basalts. *Am. Mineral.* **82,** 368–378 (1997).
22. Hilton, D. R. *et al.* Controls on magmatic degassing along the Reykjanes Ridge with implications for the helium paradox. *Earth Planet. Sci. Lett.* **183,** 43–50 (2000).
23. Honda, M. *et al.* Possible solar noble-gas component in Hawaiian basalts. *Nature* **349,** 149–151 (1991).
24. Honda, M. & McDougall, I. Primordial helium and neon in the Earth—a speculation on early degassing. *Geophys. Res. Lett.* **25,** 1951–1954 (1998).
25. Javoy, M. & Pineau, F. The volatiles record of a 'popping' rock from the Mid-Atlantic Ridge at 14° N: chemical and isotopic composition of gas trapped in the vesicles. *Earth Planet. Sci. Lett.* **107,** 598–611 (1991).
26. Moreira, M., Kunz, J. & Allègre, C. J. Rare gas systematics in popping rock: Isotopic and elemental compositions in the upper mantle. *Science* **279,** 1178–1181 (1998).
27. Sarda, P. & Graham, D. Mid-ocean ridge popping rocks: implications for degassing at ridge crests. *Earth Planet. Sci. Lett.* **97,** 268–289 (1990).
28. Ballentine, C. J., van Keken, P. E., Porcelli, D. & Hauri, E. H. Numerical models, geochemistry and the zero-paradox noble-gas mantle. *Phil. Trans. R. Soc. Lond. A* **360,** 2611–2631 (2002).
29. Holloway, J. R. Graphite-melt equilibria during mantle melting: constraints on CO_2 in MORB magmas and the carbon content of the mantle. *Chem. Geol.* **147,** 89–97 (1998).
30. Saal, A. E., Hauri, E. H., Langmuir, C. H. & Perfit, M. R. Vapour undersaturation in primitive mid-ocean-ridge basalt and the volatile content of Earth's upper mantle. *Nature* **419,** 451–455 (2002).
31. Head, J. W., Wilson, L. & Smith, D. K. Mid-ocean ridge eruptive vent morphology and substructure: Evidence for dike widths, eruption rates, and evolution of eruptions and axial volcanic ridges. *J. Geophys. Res.* **101,** 28265–28280 (1996).
32. Hilton, D. R., McMurtry, G. M. & Goff, F. Large variations in vent fluid $CO_2/^3$He ratios signal rapid changes in magma chemistry at Loihi seamount, Hawaii. *Nature* **396,** 359–362 (1998).
33. Resing, J. A., Lupton, J. E., Feely, R. A. & Lilley, M. D. CO_2 and ^{3}He in hydrothermal plumes: implications for mid-ocean ridge CO_2 flux. *Earth Planet. Sci. Lett.* **226,** 449–464 (2004).

Supplementary Information is linked to the online version of the paper at www.nature.com/nature.

Acknowledgements We thank C. Ballentine for a constructive review; M. Saar and J. Rice for providing computational resources; C. Langmuir for helpful suggestions; and R. O'Connell, S. Parman and S. Jacobsen for discussions. H.M.G. was supported by the Daly Fellowship (Department of Earth and Planetary Sciences, Harvard University).

Author Information Reprints and permissions information is available at www.nature.com/reprints. Correspondence and requests for materials should be addressed to H.M.G. (helge@hawaii.edu).